sensors

MDPI

Communication

RF-SOI Low-Noise Amplifier Using RC Feedback and Series Inductive-Peaking Techniques for 5G New Radio Application

Min-Su Kim [1] and Sang-Sun Yoo [2,*]

[1] Department of Information and Electronic Engineering, Mokpo National University, Muan 58554, Republic of Korea; msmy970@mnu.ac.kr
[2] Department of Smart Automobile, Pyeongtaek University, Pyeongtaek-si 450-701, Republic of Korea
* Correspondence: syoo@ptu.ac.kr

Abstract: This paper presents a low-noise amplifier (LNA) with an integrated input and output matching network designed using RF-SOI technology. This LNA was designed with a resistive feedback topology and an inductive peaking technology to provide 600 MHz of bandwidth in the N79 band (4.4 GHz to 5.0 GHz). Generally, the resistive feedback structure used in broadband applications allows the input and output impedance to be made to satisfy the broadband conditions through low-impedance feedback. However, feedback impedance for excessive broadband characteristics can degrade the noise performance as a consequence. To achieve a better noise performance for a bandwidth of 600 MHz, the paper provided an optimized noise performance by selecting the feedback resistor value optimized for the N79 band. Additionally, an inductive peaking technique was applied to the designed low-noise amplifier to achieve a better optimized output matching network. The designed low-noise amplifier simulated a gain of 20.68 dB and 19.94 dB from 4.4 to 5.0 GHz, with noise figures of 1.57 dB and 1.73 dB, respectively. The input and output matching networks were also integrated, and the power consumption was designed to be 9.95 mA at a supply voltage of 1.2 V.

Keywords: RF-SOI (radio frequency silicon-on-insulator); low-noise amplifier (LNA); RC feedback; inductive peaking; 5G; New Radio (NR) frequency band

Citation: Kim, M.-S.; Yoo, S.-S. RF-SOI Low-Noise Amplifier Using RC Feedback and Series Inductive-Peaking Techniques for 5G New Radio Application. *Sensors* **2023**, *23*, 5808. https://doi.org/10.3390/s23135808

Academic Editors: Shah Nawaz Burokur and Claudia Campolo

Received: 8 May 2023
Revised: 15 June 2023
Accepted: 21 June 2023
Published: 22 June 2023

1. Introduction

For the efficient utilization of the frequency spectrum, the 5G new radio frequency bands (3.3 to 4.2 GHz of N77, and 4.4 to 5.0 GHz of N79, respectively) has recently received a lot of attention, and various studies for mobile communication are being conducted for this purpose. The broadband low-noise amplifier (LNA) was designed using various design methods, and in particular, broadband low-noise amplifiers using feedback techniques have been commonly used [1–4]. Such feedback techniques have the advantage of enabling the broadband matching of the required impedance for the broadband's performance. However, it is difficult to achieve an optimized performance due to the trade-off relationship between the gain and noise performance. In addition to these methods, various design techniques, such as series peaking and gm-boosting are currently being assessed as broadband techniques [5,6].

Figure 1 shows various broadband techniques. The shunt peaking in Figure 1a adds a series resistor and inductor to compensate for the impedance drop due to the parasitic capacitance at the output [5]. This helps in reducing the rolling down of the output frequency response resulting in a broadband characteristic. However, adding a resistor creates voltage headroom, which is the limiting factor for high-voltage operations. Figure 1b displays a method using gm-boosting, which has the advantage of minimizing the sensitivity to the bandwidth and input current noise [6]. However, using larger transistors to reduce input impedance results in increased power consumption. Furthermore, the increase in parasitic capacitance from larger transistors necessitates the inclusion of additional compensation circuits to minimize its effects, thereby increasing circuit complexity.

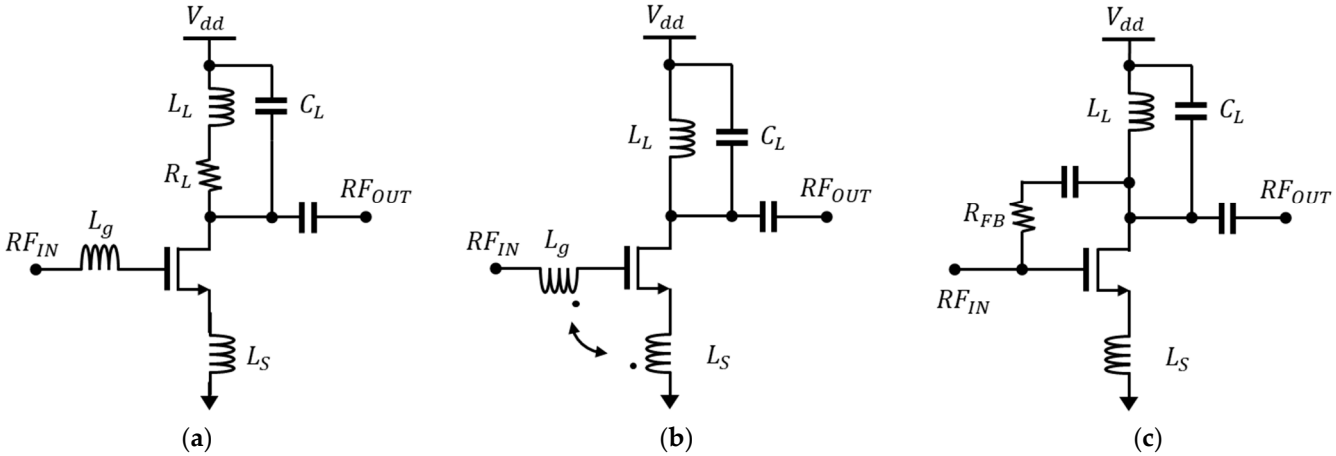

Figure 1. The broadband LNA topologies. (**a**) Inductively degenerated LNA with shunt peaking, (**b**) gm-boosted LNA, and (**c**) resistive-feedback LNA.

Figure 1c shows a commonly used structure with feedback, where matching the input impedance can be designed using the appropriate feedback resistor (R_{FB}) value [6]. However, this feedback noise cannot be arbitrarily removed, and is amplified as a result, causing the increase in the output noise, along with the occurrence of performance degradation.

In this paper, a low-noise amplifier design using an optimum RC feedback and inductive peaking technique is presented for the N79 band, covering a frequency range of 4.4 GHz to 5.0 GHz using the RF Silicon on Insulator (RF-SOI) process. To design the input and output matching network for N79 band applications, the optimal resistor value of resistive feedback was selected and subsequently optimized. In addition, an inductive peaking technique was added for the output matching network to ultimately achieve a better matching network and an optimized low-noise amplifier design. Furthermore, the proposed low-noise amplifier is designed with integrated matching networks for both input and output, enabling high integration without the need for additional external matching circuits. Section 2 presents the design methodology using resistive feedback, and Section 3 explains the inductive peaking techniques used in this paper, following which the simulation results and conclusions are presented.

2. Resistive Feedback for the Wide Input Matching Network

The resistive feedback technique has been commonly used for broadband low-noise amplifiers. However, although it can have a wideband performance according to the feedback structure, the output noise is also fed back, and is in a trade-off relationship that degrades the noise of the low-noise amplifier. Therefore, careful design consideration is necessary. Figure 2 shows a simplified circuit diagram of a Cascode low-noise amplifier with resistive feedback. Cascode LNAs have been widely used for their high gain and low-noise characteristics, including inductor (L_g) and capacitor (C_g) for matching. However, due to its narrowband characteristics, it is challenging to apply this to the broadband, meaning resistive feedback must be used to design the broadband.

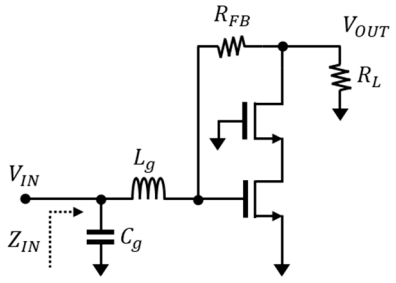

Figure 2. Simplified schematic of a Cascode low-noise amplifier.

Figure 3 illustrates an equivalent small-signal model using a common-source amplifier for the simplification of analysis. In this case, the input impedance of the LNA with feedback, including R_{FB}, can be derived as follows.

$$I_X = \frac{V_{gs} - V_{out}}{R_{FB}},\ I_X = g_m V_{gs} + \frac{V_{out}}{R_L} \tag{1}$$

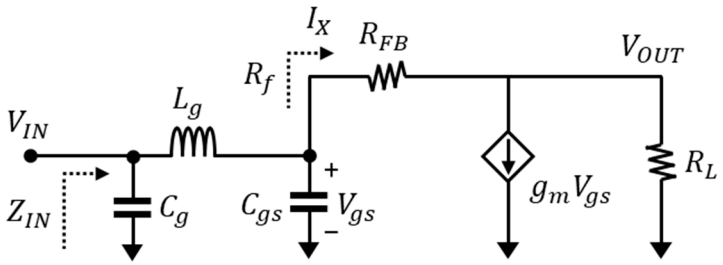

Figure 3. Simplified small-signal model of a resistive feedback common-source amplifier.

By expressing the current flowing into the R_{FB} resistor as I_x, the above equation can be obtained. C_{gs} and g_m are the gate-source capacitance and the transconductance of the transistor, respectively, and R_L is the load resistance. Using these equations, we can represent the impedance observed by the feedback as follows:

$$R_f = \frac{V_{gs}}{Ix} = \frac{R_{FB} + R_L}{1 + g_m R_L} \tag{2}$$

In this case, the intrinsic gate-drain capacitance C_{gd} was ignored. The input impedance changes due to the feedback current I_x, and this can be expressed as follows:

$$\begin{aligned} Z_{IN,w\ FB} &= \tfrac{1}{sC_g} \,||\, \left[sL_S + \left(\tfrac{1}{sC_{gs}} || R_f\right)\right] \\ &= \tfrac{1}{sC_g} || \tfrac{s^2 L_g C_{gs} R_f + sL_g + R_f}{sC_{gs} R_f + 1} = \tfrac{s^2 L_g C_{gs} R_f + sL_g + R_f}{s^3 L_g C_{gs} C_g R_f + s^2 L_g C_g + sR_f\left(C_g + C_{gs}\right) + 1} \end{aligned} \tag{3}$$

To achieve a perfect matching condition of $Z_{in} = Z_S$, it has thus been commonly assumed that $R_f = Z_S$ and $C_g = C_{gs}$. By setting C_g equal to C_{gs}, which minimizes the parasitic capacitance present in the input, and having R_f and Z_S with an equal impedance, the best matching condition can thereby be achieved. Using the given equations, we can express $|S_{11}|$ in terms of Z_{in} and Z_S, as follows:

$$|S_{11}| = \left|\frac{Z_{in} - Z_S}{Z_{in} + Z_S}\right| = \left|\frac{-s^3 L_g Z_S^2 C_{gs}^2 + s\left[L_g - Z_S^2 2C_{gs}\right]}{s^3 L_g Z_S^2 C_{gs}^2 + s^2 L_g Z_S 2C_{gs} + s\left[L_g + Z_S^2 2C_{gs}\right] + 2Z_S}\right| \tag{4}$$

where the response of $|S_{11}|$ includes two zero points. ω_{02} is as follows [7]:

$$\omega_{02} = \sqrt{\frac{2}{L_g C_{gs}} - \frac{1}{Z_S^2 C_{gs}^2}} = \frac{1}{\sqrt{L_g C_{gs}}} \tag{5}$$

where according to the condition of $L_g = R_f{}^2 C_{gs}$ and $C_g = C_{gs}$, the input matching network has a symmetrical third-order, ladder-type, low-pass filter characteristic. In this case, the frequency of ω_{02} can be adjusted using the inductance of L_g and the capacitance of C_{gs} to provide a matching condition of -10 dB or more, thereby making it possible to design a broadband matching network. However, in the case of a feedback resistor, a low impedance feedback structure cannot be applied due to the trade-off relationship between the bandwidth and the noise figure (*NF*). Therefore, optimization between the desired bandwidth for the frequency range extension and the targeted *NF* becomes essential. *NF*

can be represented using a model of the common-source amplifier with resistive feedback, which is as follows [8]:

$$NF \approx 1 + \frac{4Rs}{R_{FB}} + \gamma + \gamma g_m R_s \tag{6}$$

where γ represents the excess noise coefficient of the MOSFET. As shown in Equation (6), if the R_{FB} has a low value, the *NF* performance will degrade as a consequence. Figure 4 is a simulation result showing the relationship between the bandwidth and the *NF* according to the feedback resistor value. As the resistor value of R_{FB} decreases, the bandwidth of the input matching increases as a result. However, in the case where the NF performance degrades, the feedback resistor value used for the desired broadband matching should be matched using the optimal value.

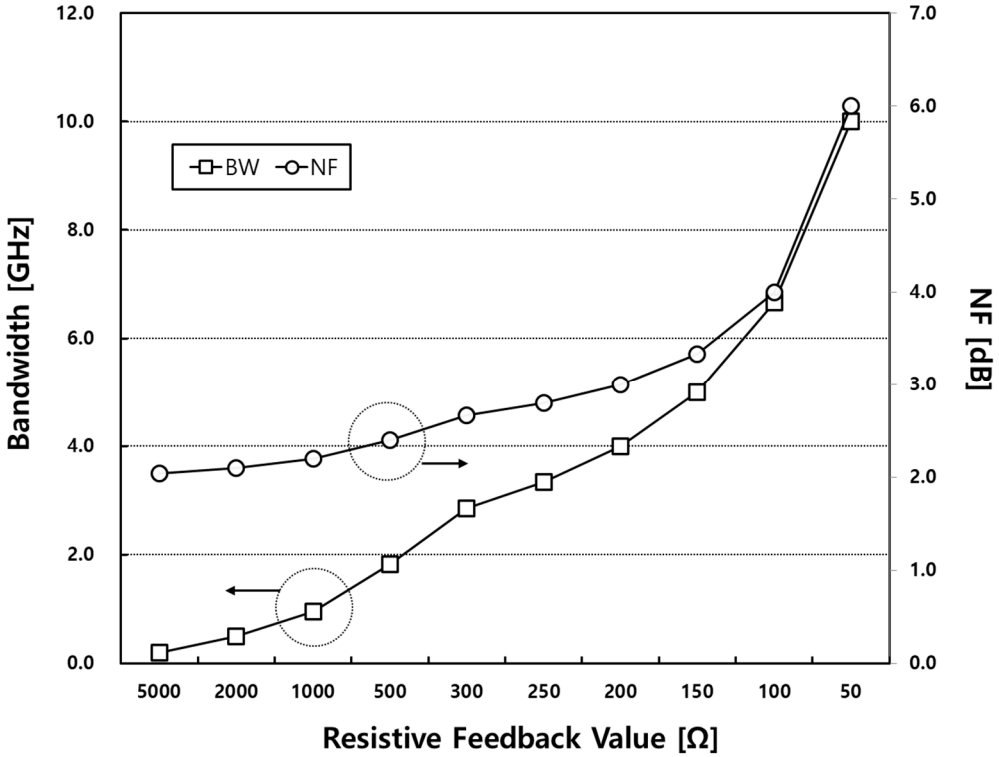

Figure 4. The simulated bandwidth and noise figure according to the resistive feedback value.

3. Inductive Peaking for the Wide Output Matching Network

Figure 5 shows the output matching network for a conventional low-noise amplifier. Here, L_L and C_L represent the frequency response characteristics of the bandpass filter, and C_{ds} is the parasitic source-drain capacitance generated in the intrinsic transistor, respectively. C_{ds} is combined with the load C_L, and together with L_L, has a resonance frequency ω_0. The impedance of the output matching network can be expressed as:

$$Z_{OUT1} = \frac{1}{sC_t} \,||\, sL_L = \frac{sL_L}{s^2 C_t L_L + 1} \tag{7}$$

As shown in Equation (7), the output impedance can be decreased depending on the C_t of the matching circuit, and due to the capacitance of C_{ds}, it will thereby have a more abrupt frequency response characteristic. C_t represents the total capacitance value of C_{ds} and C_L.

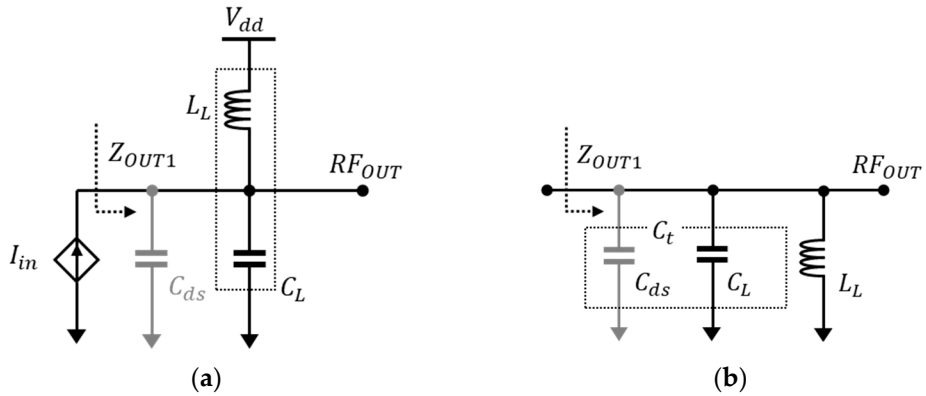

Figure 5. Conventional (**a**) output matching network and (**b**) simplification.

For the wide output matching network design, adding a series inductor L_s to the output matching network has been considered, as shown in Figure 6. The addition of a series L_s could be able to compensate for the frequency response degradation caused by the C_{ds} of the intrinsic transistor. This inductive peaking technique has been expanded to the resonance frequencies of L_s and C_{ds}, as well as to C_L and L_L, thereby allowing it to operate as a wide matching network. The output impedance can be expressed as:

$$Z_{OUT2} = \left(\frac{1}{sC_{ds}}\right) \,||\, \left(sL_s + \left[\frac{1}{sC_L} \,||\, sL_L\right]\right) = \frac{s^3 C_L L_L L_S + s(L_S + L_L)}{s^4 C_{ds} C_L L_L L_S + s^2(C_{ds} L_S + C_{ds} L_L + C_L L_L) + 1} \tag{8}$$

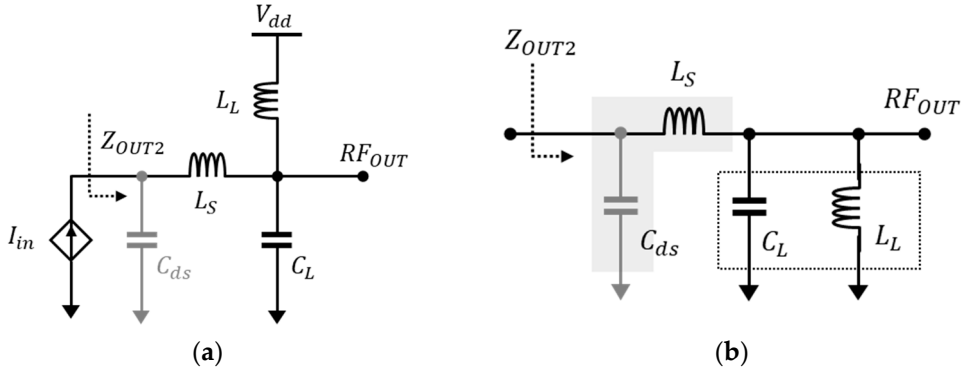

Figure 6. The (**a**) output matching network and (**b**) simplification.

When making the imaginary part of the output impedance zero, we obtain the following Equation (9), which is the characteristic equation involving the frequency ω as follows:

$$\omega^4 L_L C_L L_S C_{ds} - \omega^2 (L_S C_{ds} + L_L C_{ds} + L_L C_L) + 1 = 0 \tag{9}$$

Equation (9) can be simplified to the product of the sum of roots S and the root P, respectively, as previously shown in [9].

$$S = {\omega_1}^2 + {\omega_2}^2 = \frac{C_{ds} L_S + C_{ds} L_L + C_L L_L}{C_{ds} C_L L_L L_S} = \frac{1}{C_L L_L} + \frac{1}{C_L L_S} + \frac{1}{C_{ds} L_S} \tag{10}$$

$$P = {\omega_1}^2 {\omega_2}^2 = \frac{1}{C_{ds} C_L L_L L_S} \tag{11}$$

Using Equations (10) and (11), we can determine three resonance frequencies through the output matching network: $\omega_{1,\,2}$, and the average of the two operating radian frequencies, which hence referred to as ω_3. The ω_3 resonance frequency can be determined using the ratio of L_S to L_L and C_L to C_{ds}, respectively, and the network should be designed with an optimal matching value to achieve the desired performance.

4. Low-Noise Amplifier Design for the NR 79 Band

Figure 7a shows a Cascode low-noise amplifier, which uses the resistive feedback structure and an inductive peaking technique for the N79 band. The decoupling capacitors C_g, C_{FB}, and C_{out}, were all added to the design. C_{total} is an equivalent capacitance that represents the combination of parasitic capacitance from the Electrostatic Discharge (ESD) protection circuit and bump pad and was designed to be included in the input matching network. In the previous section, C_{total}, similar to C_g in Figure 5, is a parameter that needs to be taken into consideration, as it can unexpectedly affect the matching conditions.

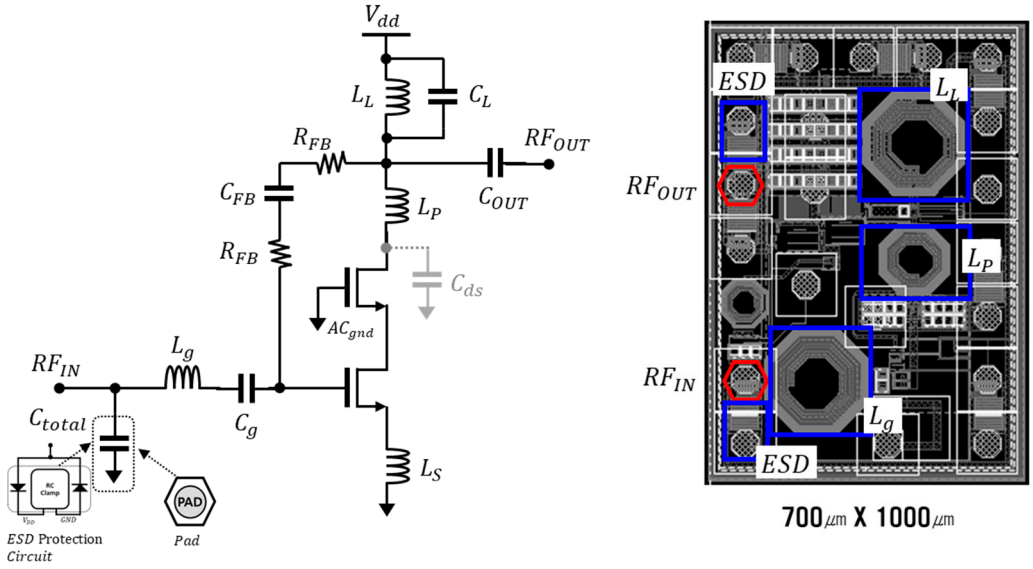

(**a**) (**b**)

Figure 7. The (**a**) Schematic and (**b**) layout of the designed LNA.

In a real design, resistors are accompanied with parasitic parallel capacitors that are generated in the layout. This parasitic parallel capacitor is a capacitor between the metal line for connection and the substrate, and the larger the resistance, the larger the parasitic capacitor that is formed. Therefore, to achieve the same effect for the output and input in the feedback structure, the resistive feedback (R_{FB}) was symmetrically applied with a decoupling capacitor to achieve the required resistance for the resistive feedback structure. C_{ds} represents the capacitance generated at the drain of the common-gate transistor in the Cascode amplifier. As C_{ds} performs a function that causes a faster rolling down depending on the frequency in the general output matching network, L_P was added as a compensation. Then, the output matching with the third pole was designed with L_L and C_L. Figure 7b represents the chip layout of the designed LNA, which was designed at a size of 700 μm × 1000 μm and includes a ESD protection circuit for the input and output, as well as three matching inductors for impedance matching. Furthermore, the layout includes ground bumps for the AC grounding of the common-gate stage.

The designed LNA was implemented using the GlobalFoundries RF-SOI 90 nm process. The widths of the two transistors were designed to be 128 μm, and the sum of the synthetic resistor of feedback resistors was 7 k ohm to achieve the desired gain and NF performance, respectively. A small degeneration inductor, Ls, was added to the 120 pH inductor to obtain better matching conditions. Figure 8 shows the simulation results of the LNA for the N79 band. The LNA consumes a current of 9.95 mA at a 1.2 V supply voltage. Figure 8a shows the forward gain S_{21}, input, and output reflection coefficients (S_{11} and S_{22}, respectively). Figure 8b presents the simulated results of the NF and NF_{min} up to 5.4 GHz. The LNA exhibited a gain of 20.68 dB at 4.4 GHz with the input and output reflection coefficients of −9.24 dB and −15 dB, respectively. At 5.0 GHz, it exhibited a gain of 19.94 dB, with the input and output reflection coefficients of −12.6 dB and −14.6 dB, respectively.

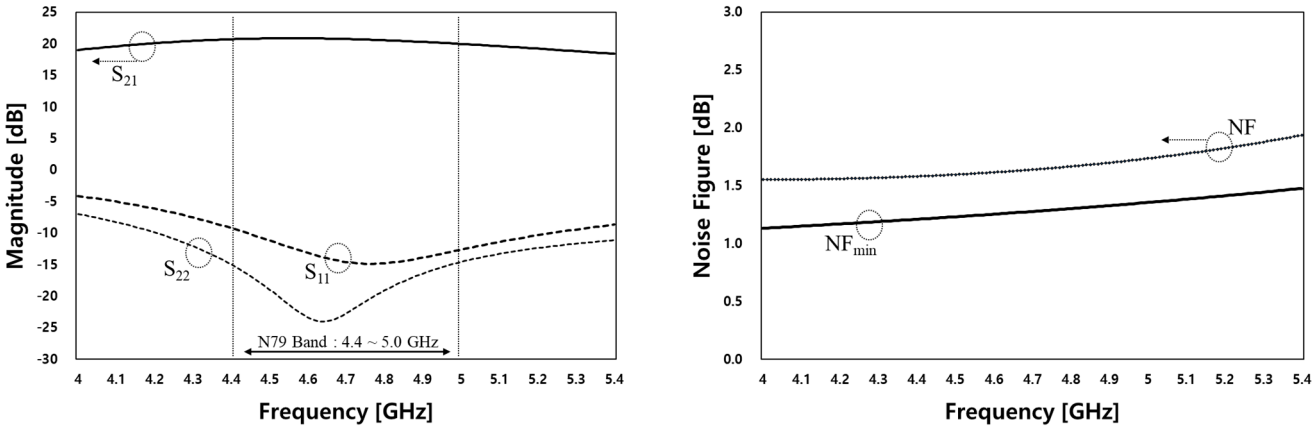

(**a**) (**b**)

Figure 8. Simulated (**a**) S_{21}, S_{11}, and S_{22}, and (**b**) NF and NFmin performance.

The simulated NF was determined to be 1.57 dB and 1.73 dB, with NF_{min} values of 1.2 dB and 1.32 dB at 4.4 GHz and 5.0 GHz, respectively. This paper applied resistive feedback for designing an LNA operating in the N79 band. Although the designed LNA achieved a bandwidth of 600 MHz, it was designed with a performance difference of around 0.38 dB from the optimal low-noise performance, NF_{min}, as shown in Figure 7b. However, it has the advantage of including an internal input/output matching network, which shows an excellent performance from the point of view of the NF. This is because the inductor used in typical chip internal matching networks may cause degradation in the noise performance with a relatively low Q value but may still have an advantage in terms of size in a circuit configuration for an external matching circuit.

In Figure 9, the input third-order intercept point (IIP_3) was simulated to be −15.4 dBm at 1 MHz tone spacing. The LNA using feedback generally exhibited an improved linearity compared to the conventional LNAs, as the feedback had a greater effect on the high power obtained from the input.

A summary of the results is provided in Table 1. Generally, LNAs using resistive feedback possess wide broadband characteristics. However, this paper presents an optimized LNA design for the N79 band using appropriate resistive feedback and inductive peaking techniques, rather than a typical broadband LNA design. Therefore, it was compared with previous studies which assessed in the 0.2 to 5 GHz band. As shown in Table 1, the designed LNA satisfies the bandwidth requirement for the N79 band and exhibits excellent performance in terms of the NF and IIP_3.

Table 1. LNA performance summary and comparison.

Ref.	Technology	Frequency [GHz]	S_{11}/S_{22} [dB]	Gain [dB]	NF [dB]	IIP_3 [dBm]	Area [mm^2]
[10]	180 nm CMOS	3–5	<−10.5/-	16	1.8	−9	0.63
[11]	65 nm CMOS	0.2–5	-/-	15.6	<3.5	>0	0.009
[12]	180 nm RFSOI	5	−33/−28	11	0.95	5	0.29
	180 nm RFSOI	5	−22/−28	9.3	1.9	6.5	0.29
This work *	90 nm RFSOI	4.4–5.0	−9.4/−15	20.6–19.9	1.57–1.73	−15.4	0.7

* Simulation results.

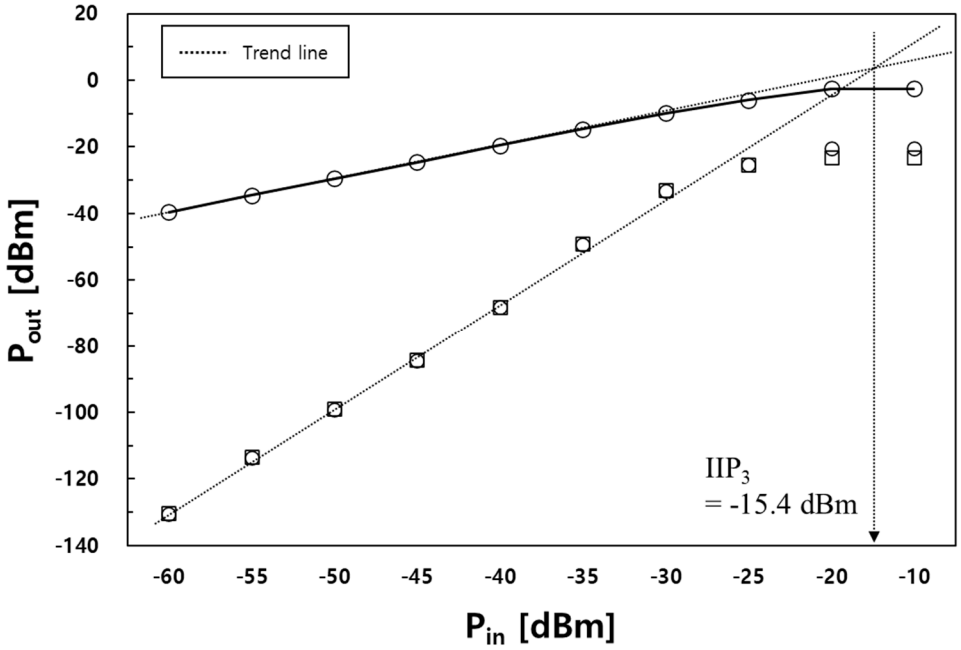

Figure 9. Simulated output power with respect to the input power.

5. Conclusions

This paper presents the design of a low-noise amplifier using the RF-SOI process. The designed low-noise amplifier applied resistive feedback and an inductive peaking technique for the N79 band operation. Although the additional inductive peaking technique includes an increase in the chip size, this paper integrated the matching network that needs to be used externally to eliminate the additional external matching components. In addition, to minimize the occurrence of errors between the design and measurements, circuit design was performed with EM-based simulation results and the PEX-based model. This low-noise amplifier was designed and simulated to achieve an optimal performance for a bandwidth of 600 MHz, and these broadband techniques can be appropriately applied to various low-noise amplifier designs.

Author Contributions: Conceptualization, M.-S.K. and S.-S.Y.; methodology, M.-S.K.; software, M.-S.K.; validation, M.-S.K. and S.-S.Y.; formal analysis, M.-S.K.; investigation, M.-S.K.; resources, M.-S.K.; data curation, M.-S.K.; writing—original draft preparation, M.-S.K.; writing—review and editing, S.-S.Y.; visualization, S.-S.Y.; supervision, S.-S.Y.; project administration, M.-S.K.; funding acquisition, M.-S.K. All authors have read and agreed to the published version of the manuscript.

Funding: This research was supported by the Research Funds of Mokpo National University in 2022, grant number 2022-0382.

Institutional Review Board Statement: Not applicable.

Informed Consent Statement: Not applicable.

Data Availability Statement: Not applicable.

Conflicts of Interest: The authors declare no conflict of interest.

References

1. Balteanu, F.; Modi, H.; Choi, Y.; Lee, J.; Drogi, S.; Khesbak, S. 5G RF front end module architectures for mobile applications. In Proceedings of the 2019 49th European Microwave Conference (EuMC), Paris, France, 1–3 October 2019; IEEE: Piscataway, NJ, USA, 2019; pp. 252–255.
2. Li, C.; Wang, M.; Chi, T.; Kumar, A.; Boenke, M.; Wang, D.; Cahoon, N.; Bandyopadhyay, A.; Joseph, A.; Wang, H. 5G mm-wave front-end-module design with advanced SOI process. In Proceedings of the IEEE 12th International Conference on ASIC (ASICON), Guiyang, China, 25–28 October 2017; pp. 1017–1020.

3. Dai, R.; Ren, J.; He, J.; Xiao, J.; Kong, W. RFFE integration design for 5g in 0.13 um RFSOI technology. In Proceedings of the 2019 China Semiconductor Technology International Conference (CSTIC), Shanghai, China, 18–19 March 2019; pp. 1–3.
4. Perumana, B.G.; Zhan, J.C.; Taylor, S.S.; Carlton, B.R.; Laskar, J. Resistive-Feedback CMOS Low-Noise Amplifiers for Multiband Applications. *IEEE Trans. Microw. Theory Tech.* **2008**, *56*, 1218–1225.
5. Xiong, Y.; Zeng, X.; Wang, G.; Liu, C. A Compact 4~8 GHz Low Noise Amplifier MMIC with Standing-By Feature for 5G Communication Applications. In Proceedings of the 2019 3rd International Conference on Electronic Information Technology and Computer Engineering (EITCE), Xiamen, China, 18–20 October 2019; pp. 394–397.
6. Joo, S.; Choi, T.; Jung, B. A 2.4-GHz Resistive Feedback LNA in 0.13 µm CMOS. *IEEE J. Solid-State Circuits* **2009**, *44*, 3019–3029. [CrossRef]
7. Wu, J.; Liu, Z. A 40 nm CMOS UltraWideband Low Noise Amplifier Design, Advances in Computer Science Research. In Proceedings of the International Conference on Wireless Communication, Network and Multimedia Engineering (WCNME 2019), Guilin, China, 21–22 April 2019; Volume 89.
8. Razavi, B. *RF Microelectronics (2nd Edition) (Prentice Hall Communications Engineering and Emerging Technologies Series)*, 2nd ed.; Prentice Hall Press: Upper Saddle River, NJ, USA, 2011; ISBN 978-0-13-713473-1.
9. Datta, S.; Datta, K.; Dutta, A.; Bhattacharyya, T.K. Fully concurrent dual-band LNA operating in 900 MHz/2.4 GHz bands for multi-standard wireless receiver with sub-2 dB noise figure. *Int. Emerg. Trends Eng. Conf. Tech. Dig.* **2010**, *1*, 731–734.
10. Lee, H.-J.; Ha, D.S.; Choi, S.S. A 3–5 GHz CMOS UWB LNA with input matching using miller effect. In Proceedings of the IEEE International Solid-State Circuits Conference, San Francisco, CA, USA, 6–9 February 2006.
11. Blaakmeer, S.C.; Klumperink, E.A.M.; Leenaerts, D.M.W.; Nauta, B. Wideband Balun-LNA with Simultaneous Output Balancing, Noise-Canceling and Distortion-Canceling. *IEEE J. Solid-State Circuits* **2008**, *43*, 1341–1350. [CrossRef]
12. Madan, A.; McPartlin, M.J.; Masse, C.; Vaillancourt, W.; Cressler, J.D. A 5 GHz 0.95 dB NF Highly Linear Cascode Floating-Body LNA in 180 nm SOI CMOS Technology. *IEEE Microw. Wirel. Compon. Lett.* **2012**, *22*, 200–202. [CrossRef]